

Research Article

Atomic Marginal Distribution and Squeezing Phenomena of Correlated Two Modes Interacting with a Three-Level Atom in the Presence of an External Classical Field

A.-S. F. Obada,¹ E.M. Khalil ,² S. Sanad,³ and H.F. Habeba⁴

¹Mathematics Department, Faculty of Science, Al-Azhar University, Nasr City 11884, Cairo, Egypt

²Department of Mathematics, College of Science, Taif University, P.O. Box 11099, Taif 21944, Saudi Arabia

³Mathematics Department, Faculty of Science (Girls Branch), Al-Azhar University, Nasr City 11884, Cairo, Egypt

⁴Department of Mathematics and Computer Science, Faculty of Science, Menoufia University, Shebin Elkom 32511, Egypt

Correspondence should be addressed to E.M. Khalil; eiedkhalil@yahoo.com

Received 2 March 2022; Revised 22 May 2022; Accepted 31 May 2022; Published 30 June 2022

Academic Editor: Yuan-Fong Chou Chau

Copyright © 2022 A.-S. F. Obada et al. This is an open access article distributed under the Creative Commons Attribution License, which permits unrestricted use, distribution, and reproduction in any medium, provided the original work is properly cited.

The influence of the external classical field on a correlated two-mode of the electromagnetic field interacting with a three-level atom in the Λ structure is studied. A rotation of the atomic basis is used to remove the classical field terms. The time-dependent wave function is obtained by solving the Schrödinger equation. The influence of the classical field on the phenomenon of revival, collapse, squeezing, and marginal atomic distribution are discussed. In our analysis, the cavity field is prepared in the entangled pair coherent states and the atomic system in the upper state. The results showed that the occupation of the atomic level is significantly affected by the addition of the classical field. The presence of the classical field reduces the squeezing intervals and the extreme values of the atomic marginal distribution.

1. Introduction

The effects of the interaction between an atom and a quantized field are fundamental problems in quantum information. Several models have been proposed to describe this interaction, and one of the most famous of these is the Jaynes-Cummings model (JCM) [1]. This model is the most important model in quantum information, where, it is solved exactly using the rotating wave approximation (RWA) and has been experimentally implemented [2]. There are a number of generalizations of the JCM, such as multilevel atom [3–6], multiphoton transition [7], and multimode field [8].

The multimode in electromagnetic field performs an important role in various quantum optics applications. One of the most important multimode states is the entangled pair coherent states, which represents a correlated two-mode state [9]. There are several papers devoted to using paired coherent states, such as an

interaction of the atomic system with a correlated two-mode coherent state that has been discussed [10]. The two two-level atoms interacting with a two-mode field has been studied, where the cavity field is prepared in the squeezed-pair coherent state [11]. Also, the problem of a parameter estimation in a qubit interacting with a two-mode field has been investigated, with the two modes correlated [12]. The effect of two modes of the cavity field on the interaction of a two-level atom in the presence of amplifier terms was studied [13]. The effect of Kerr medium and the temperature on the interaction of two two-level entangled atoms containing two levels with a single-mode quantum electromagnetic field in a cavity via the two-photon degenerate transition was addressed [14].

There are many applications for the interaction of a three-atom with the mechanical effects of a laser field. The atomic aberration of both Λ -type and V -type atoms interacting with entangled light waves was investigated [15]. The evolution of temperatures over time below the Doppler limit

was predicted when three-level atoms from Λ -type are cooled in a high-quality optical cavity [16]. A study was presented on the placement of three paired atomic traps through the tunnels, which showed an analogy with a three-level Λ -type atom irradiating with two laser beams [17]. The three-level atom diagram has been studied as a candidate for creating artificial measurement capabilities for neutral atoms. In this case, the motion of the center of mass simulates the dynamics of a charged particle in a magnetic field with the appearance of a Lorentz-like force [18].

The study of the effect of the external classical field (ECF) on some physical determinants has attracted the interest of many researchers to study the entanglement between quantum systems. Some nonclassical properties, for example, the revivals and collapses phenomenon (RCP), squeezing phenomenon, quasi-probability distribution, etc., have also been studied in different structures [19]. The influence of ECF on entanglement, RCP, and squeezing phenomenon has been discussed on JCM [20]. Also, the effect of phase damping and ECF on JCM has been discussed [21]. A two-level atom interacting with an N-level atom model has been studied in the presence of ECF [22]. The effect of ECF and nonlinear medium on the two-level atom interacting with an electromagnetic field has been discussed [23]. Also, the effect of ECF on the geometric phase and squeezing phenomenon of two two-level atoms interacting with N-level atom has been illustrated [24]. Finally, the effects of ECF and the detuning parameter on the RCP, squeezing phenomenon, atomic Q-function, and atomic Wehrl density for the interaction between SU(1,1) quantum system and a three-level atom have been investigated [25]. The dissipation effect of the external field on deformed two identically atoms was studied [26, 27].

The aim of this work is to study the interaction of a correlated two-mode of electromagnetic field with a three-level atom. Also, it aims to study the effect of ECF on RCP, squeezing phenomenon, and atomic Wehrl density.

This paper is organized as follows: in the following section, the description of the investigated model and its solution are presented. In Section 3, the revivals and collapses phenomenon is discussed. The squeezing phenomenon is studied in Section 4 and Section 5. We discuss the atomic marginal distribution in Section 6. Finally, some brief remarks are given in Section 7. (see Figure 1

2. The Description of the Model and Its Solution

This section presents the effect of ECF on a quantum model containing a cavity-filled field with two correlated modes interacting with a three-level atom in the Λ -configuration. Therefore, the total Hamiltonian describing this model takes the subsequent form [25],

$$\hat{H} = \hat{H}_0 + \hat{H}_1 + \hat{H}_2 + \hat{H}_3, \quad (1)$$

where \hat{H}_0 represents the Hamiltonian of the free system, and it can be written as follows:

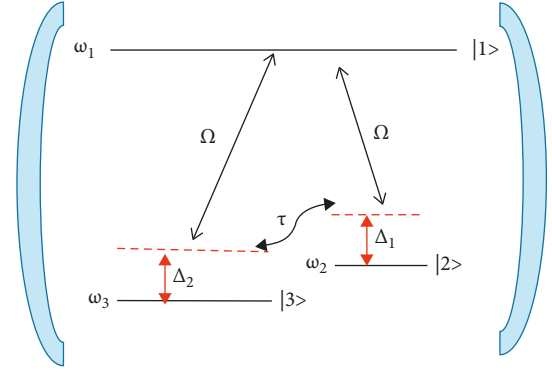


FIGURE 1: A sketch of the three-level atom in the Λ -configuration located inside a cavity field with an external classical field. Here, ω_1 , ω_2 , and ω_3 are the frequencies of the levels, Ω is the frequency of the quantized cavity field, and τ is the frequency of the external classical field.

$$\hat{H}_0 = \frac{\Omega}{2} (\hat{n}_a + \hat{n}_b + 1) + \omega_1 |1\rangle\langle 1| + \omega_2 |2\rangle\langle 2| + \omega_3 |3\rangle\langle 3|. \quad (2)$$

\hat{H}_1 and \hat{H}_2 are the interaction Hamiltonian, which are given by the following:

$$\hat{H}_1 = i\omega (\hat{a}^\dagger \hat{b}^\dagger + \hat{a}\hat{b}) (|1\rangle\langle 3| - |3\rangle\langle 1|), \quad (3)$$

$$\hat{H}_2 = i\omega (\hat{a}^\dagger \hat{b}^\dagger + \hat{a}\hat{b}) (|1\rangle\langle 2| - |2\rangle\langle 1|). \quad (4)$$

The ECF Hamiltonian can be written as follows:

$$\hat{H}_3 = \tau (|2\rangle\langle 3| + |3\rangle\langle 2|), \quad (5)$$

where Ω represents the frequency of the field. ω_α with $\alpha \in \{1, 2, 3\}$ represents the atomic frequencies with $\omega_1 > \omega_2 > \omega_3$. The operators \hat{a} and \hat{b} are the boson operators that satisfy the commutation relation, $[\hat{a}, \hat{b}] = 0$, $[\hat{a}, \hat{a}^\dagger] = 1$, $[\hat{b}, \hat{b}^\dagger] = 1$, and $\hat{n}_a = \hat{a}^\dagger \hat{a}$, $\hat{n}_b = \hat{b}^\dagger \hat{b}$. ω is the coupling constant parameter, and τ represents the ECF coupling parameter.

Our goal in this paper is to study the influence of ECF on some statistical properties. Hence, we need to solve the Hamiltonian (1).

Firstly, the unitary transformation is introduced to simplify the Hamiltonian (1).

$$\begin{pmatrix} |1\rangle \\ |2\rangle \\ |3\rangle \end{pmatrix} = \begin{pmatrix} 1 & 0 & 0 \\ 0 & \cos(\varepsilon) & \sin(\varepsilon) \\ 0 & -\sin(\varepsilon) & \cos(\varepsilon) \end{pmatrix} \begin{pmatrix} |e\rangle \\ |i\rangle \\ |g\rangle \end{pmatrix}, \quad (6)$$

where $\varepsilon = 1/2 \arctan(2\tau/\omega_3 - \omega_2)$.

By applying the conical transformation into (1) and applying RWA, the transformed Hamiltonian can be written as follows:

$$\hat{H} = \hat{H}_1 + \hat{H}_2, \quad (7)$$

where

$$\hat{H}_1 = \frac{\Omega}{2} (\hat{n}_a + \hat{n}_b + 1) + \omega_1 |e\rangle \langle e| + \bar{\Omega}_i |i\rangle \langle i| + \bar{\Omega}_g |g\rangle \langle g|, \quad (8)$$

$$\begin{aligned} \hat{H}_2 = & i\gamma_1 (\hat{a}\hat{b}|e\rangle \langle i| - \hat{a}^\dagger \hat{b}^\dagger |i\rangle \langle e|) \\ & + i\gamma_2 (\hat{a}\hat{b}|e\rangle \langle g| - \hat{a}^\dagger \hat{b}^\dagger |g\rangle \langle e|), \end{aligned} \quad (9)$$

with

$$\bar{\Omega}_i = \omega_2 \cos^2(\varepsilon) + \omega_3 \sin^2(\varepsilon) - \tau \sin(2\varepsilon), \quad (10)$$

$$\bar{\Omega}_g = \omega_3 \cos^2(\varepsilon) + \omega_2 \sin^2(\varepsilon) + \tau \sin(2\varepsilon), \quad (11)$$

$$\gamma_1 = \bar{\omega} (\cos(\varepsilon) - \sin(\varepsilon)), \quad (12)$$

$$\gamma_2 = \bar{\omega} (\cos(\varepsilon) + \sin(\varepsilon)). \quad (13)$$

Now, we obtain the interaction picture $\hat{H}_{int} = \exp(i\hat{H}_1 t) \hat{H}_2 \exp(-i\hat{H}_1 t)$ of the Hamiltonian (7) to find the exact solution of this system.

It can be written as follows:

$$\begin{aligned} \hat{H}_{int} = & i\gamma_1 (\hat{a}\hat{b}e^{i\Delta_1 t} |e\rangle \langle i| - \hat{a}^\dagger \hat{b}^\dagger e^{-i\Delta_1 t} |i\rangle \langle e|) \\ & + i\gamma_2 (\hat{a}\hat{b}e^{-i\Delta_2 t} |e\rangle \langle g| - \hat{a}^\dagger \hat{b}^\dagger e^{i\Delta_2 t} |g\rangle \langle e|), \end{aligned} \quad (14)$$

where, Δ_α , ($\alpha = 1, 2$) represents the detuning parameters, and they are defined as follows:

$$\Delta_1 = -\Omega - (\bar{\Omega}_i - \omega_1), \quad (15)$$

$$\Delta_2 = \Omega - (\omega_1 - \bar{\Omega}_g). \quad (16)$$

Assuming that the atom starts from the upper-most state ($|e\rangle$) while the field is prepared in the entangled pair coherent states ($|\xi, q\rangle$) [9], the initial wave state of the system is given by the following:

$$|\psi(0)\rangle = |e\rangle \otimes |\xi, q\rangle, \quad (17)$$

$$|\xi, q\rangle = N_q \sum_{m=0}^{\infty} \frac{\xi^m}{\sqrt{m!(m+q)!}} |m+q, m\rangle, \quad (18)$$

where

$$N_q = \sum_{m=0}^{\infty} [|\xi|^{2m}/m!(m+q)!]^{(-1)/2}$$

The wave function of the whole system (7) at $t > 0$ takes the following form:

$$\begin{aligned} |\psi(t)\rangle = & \sum_{m=0}^{\infty} [X_1(m, t)|e, q+m, m\rangle + X_2(m, t)|i, q+m \\ & + 1, m+1\rangle + X_3(m, t)|g, q+m+1, m+1\rangle], \end{aligned} \quad (19)$$

where the coefficients $X_i(m, t)$, ($i = 1, 2, 3$) are the probability amplitudes. They satisfy $\sum_{i=1}^3 |X_i(m, t)|^2 = 1$. $X_i(m, t)$, ($i = 1, 2, 3$) are obtained by solving the following

system of differential equations, which is given by Schrödinger's equation $i(\partial/\partial t)|\psi(t)\rangle = \hat{H}_{int}|\psi(t)\rangle$,

$$i \frac{d}{dt} X_1(m, t) = \prod_1 e^{i\Delta_1 t} X_2(m, t) + \prod_2 e^{-i\Delta_2 t} X_3(m, t), \quad (20)$$

$$i \frac{d}{dt} X_2(m, t) = -\prod_1 e^{-i\Delta_1 t} X_1(m, t), \quad (21)$$

$$i \frac{d}{dt} X_3(m, t) = -\prod_2 e^{i\Delta_2 t} X_1(m, t), \quad (22)$$

where

$$\Pi_1 = i\gamma_1 \sqrt{m+1} \sqrt{q+m+1}, \quad (23)$$

$$\Pi_2 = i\gamma_2 \sqrt{m+1} \sqrt{q+m+1}. \quad (24)$$

By writing $X_2(m, t) = e^{i\mu t}$ in Eqs.(20), (21), and (22), we obtain the following:

$$\mu^3 + \iota_1^2 \mu + \iota_2 \mu + \iota_3 = 0, \quad (25)$$

where

$$\iota_1 = 2\Delta_1 + \Delta_2 \quad (26)$$

$$\iota_2 = \Delta_1^2 + \Delta_1 \Delta_2 + \Pi_1^2 + \Pi_2^2, \quad (27)$$

$$\iota_3 = \Pi_1^2 (\Delta_1 + \Delta_2). \quad (28)$$

The solution of the third order equation is as follows:

$$\mu_j = \frac{-1}{3} \iota_1 + \frac{2}{3} \sqrt{\iota_1^2 - 3\iota_2} \cos\left(\chi + \frac{2}{3}(j-1)\pi\right), \quad (j = 1, 2, 3), \quad (29)$$

where

$$\chi = \frac{1}{3} \cos^{-1} \left(\frac{-2\iota_1^3 + 9\iota_1 \iota_2 - 27\iota_3}{2(-3\iota_2 + \iota_1^2)^{3/2}} \right). \quad (30)$$

$X_2(m, t)$ can be written as a linear combination of $e^{i\mu_j t}$ as follows:

$$X_2(m, t) = \prod_1 \sum_{j=1}^3 a_j e^{i\mu_j t}. \quad (31)$$

By inserting Eq. (31) in the differential equations (20)–(22) and after some straightforward calculations, $X_j(m, t)$, $j = 1, 2, 3$ are given as follows:

$$X_1(m, t) = \sum_{j=1}^3 b_j \mu_j e^{i(\mu_j + \Delta_1)t}, \quad (32)$$

$$X_2(m, t) = \prod_1 \sum_{j=1}^3 b_j e^{i\mu_j t}, \quad (33)$$

$$X_3(m, t) = \frac{-1}{\Pi_2} \sum_{j=1}^3 b_j (\mu_j (\mu_j + \Delta_1) + \Pi_1^2) e^{i(\mu_j + \Delta_1 + \Delta_2)t}, \quad (34)$$

where the coefficient b_α , ($\alpha = 1, 2, 3$) depends on the initial condition of the system.

Now, the wave function of system (1) takes the following form:

$$|\Phi(t)\rangle = \sum_{m=0}^{\infty} [Y_1(m, t)|1, m+q, m\rangle + Y_2(m, t)|2, m+q+1, m+1\rangle + Y_3(m, t)|3, m+q+1, m+1\rangle], \quad (35)$$

where

$$Y_1(m, t) = X_1(m, t), \quad (36)$$

$$Y_2(m, t) = X_2(m, t)\cos(\varepsilon) + X_3(m, t)\sin(\varepsilon), \quad (37)$$

$$Y_3(m, t) = -X_2(m, t)\sin(\varepsilon) + X_3(m, t)\cos(\varepsilon). \quad (38)$$

The atomic density operator $\hat{\rho}_{\text{atom}}(t)$ is given as follows:

$$\hat{\rho}_{\text{atom}}(t) = Tr_{\text{field}}|\Phi(t)\langle\Phi(t)|, \quad (39)$$

$$\hat{\rho}_{\text{atom}}(t) = \begin{pmatrix} \wp_{11}(t) & \wp_{12}(t) & \wp_{13}(t) \\ \wp_{21}(t) & \wp_{22}(t) & \wp_{23}(t) \\ \wp_{31}(t) & \wp_{32}(t) & \wp_{33}(t) \end{pmatrix}. \quad (40)$$

Some nonclassical properties of the proposed system (1) are discussed in the forthcoming sections, where we can analyze the effect of the ECF in the present system.

3. The Revivals and Collapses Phenomenon

In this section, the effect of ECF on RCP for the Hamiltonian (1) using the definition of the atomic inversion is studied. It is defined as the difference between the atomic levels occupation, which is given as follows:

$$W(t) = \wp_{11}(t) - ((\wp_{22}(t) + \wp_{33}(t))). \quad (41)$$

Atomic inversion is described after defining the parameters $\omega = 0.3, q = 3, \xi = 16$. From equations (15) and (16), in the case of resonance, the classical field effect does not appear. That is because $\Delta_1 = \Delta_2 = 0$, and therefore, the coupling parameter τ becomes $\tau = |\omega_2 - \omega_3|/2$. In Figures 2(a), 3(a), the external field is excluded, and the resonance case is considered. The function $W(t)$ is symmetric about the horizontal axis. RCP are frequently realized. The numerical results showed that the atom loses energy during the collapse period and also gains energy during the period of revival. When adding detuning to the cavity (nonresonance case), RCP disappears completely. Moreover, the horizontal axis of symmetry is shifted down. This result confirms that the atom has lost its energy. Therefore, it fluctuates almost around the lower level. Moreover, the maximum values of the oscillations decrease

greatly in the nonresonance case, as evident from Figure 2(b). The atom stores energy after the ECF has inserted. Therefore, the axis of symmetry of the function $W(t)$ returns about 0 again. It indicates that the existence of the ECF improves the realization of the RCP (see Figure 2(c)). As the ECF effect increases, the amount of energy stored increases, which causes the axis of symmetry to shift upward. Moreover, the atomic inversion fluctuates around the upper level most of the interaction times. RCP is clearly improved by increasing the ECF as observed in Figures 2(d) and 3(b).

Here, the effect of ECF on the occupation of the three-level atom is analyzed. Firstly, by excluding ECF, the third and second levels have same behavior, while the first level is shifted up as seen in the Figure 4(a). In addition to that, RCP is formed in a periodic manner. After the inclusion of ECF, regular oscillations are generated during the periods of collapse. The results also indicate that the first level is not affected, while ECF strongly affects the second and third levels (see Figure 4(b)). The presence of ECF increases energy storage at the level for some periods and reduces energy storage at other periods.

4. Entropy Squeezing

The inequality of the entropic uncertainty inequality for $n+1$ complementary observables is given by [28, 29].

$$\sum_{\beta=1}^{n+1} H(\hat{L}_\beta) \geq n \ln \left[\frac{1}{2} (n+1) \right], \quad (42)$$

where this inequality is achieved only in a prime n -dimensional Hilbert space.

$H(\hat{L}_\beta)$ represent the Shannon information entropics. They are defined as follows:

$$H(\hat{L}_\beta) = - \sum_{\alpha=1}^n R_\alpha(\hat{L}_\beta) \ln R_\alpha(\hat{L}_\beta), \quad \beta = x, y, z, \quad (43)$$

where $R_\alpha(\hat{L}_\beta)$ indicates the probability distribution of the n possible outcomes for measurements of the \hat{L}_β operator.

For a three-level atom, $R_\alpha(\hat{L}_\beta)$ can be written as follows [25, 30]:

$$R_1(\hat{L}_x) = \frac{1}{2} (\wp_{11}(t) - 2\text{Re}[\wp_{13}(t)] + \wp_{33}(t)), \quad (44)$$

$$R_2(\hat{L}_x) = \frac{1}{4}\wp_{11}(t) + \frac{1}{\sqrt{2}}\text{Re}[\wp_{12}(t)] + \frac{1}{2}\wp_{22}(t) + \frac{1}{2}\text{Re}[\wp_{13}(t)] + \frac{1}{\sqrt{2}}\text{Re}[\wp_{23}(t)] + \frac{1}{4}\wp_{33}(t), \quad (45)$$

$$R_3(\hat{L}_x) = \frac{1}{4}\wp_{11}(t) - \frac{1}{\sqrt{2}}\text{Re}[\wp_{12}(t)] + \frac{1}{2}\wp_{22}(t) + \frac{1}{2}\text{Re}[\wp_{13}(t)] - \frac{1}{\sqrt{2}}\text{Re}[\wp_{23}(t)] + \frac{1}{4}\wp_{33}(t), \quad (46)$$

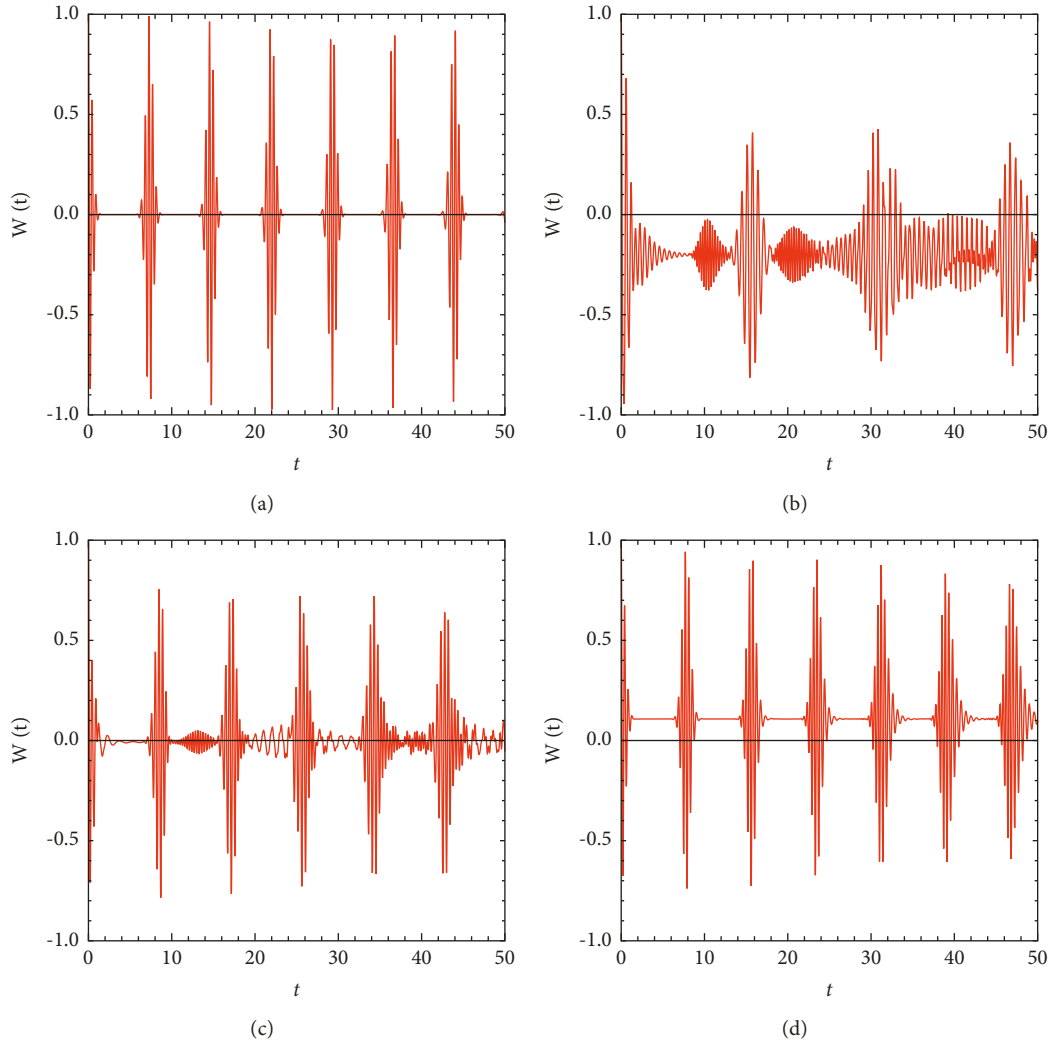


FIGURE 2: $W(t)$ as a function of the scaled time t , with, $\omega = 0.3, q = 3, \xi = 16$. (a) $\Delta_1 = \Delta_2 = 0, \tau = 0$, (b) $\Delta_1 = 5, \Delta_2 = 10, \tau = 0$, (c) $\Delta_1 = 5, \Delta_2 = 10, \tau = 0.2$, (d) $\Delta_1 = 5, \Delta_2 = 10, \tau = 1$.

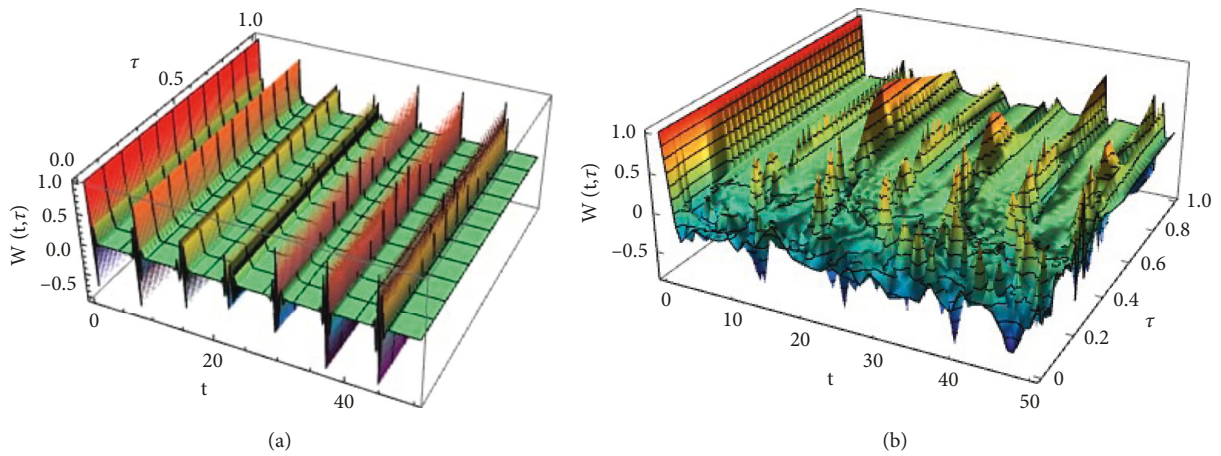


FIGURE 3: $W(t, \tau)$ as a function of the scaled time t and the classical field parameter τ , with, $\omega = 0.3, q = 3, \xi = 16$, (a) $\Delta_1 = \Delta_2 = 0$, (b) $\Delta_1 = 5, \Delta_2 = 10$.

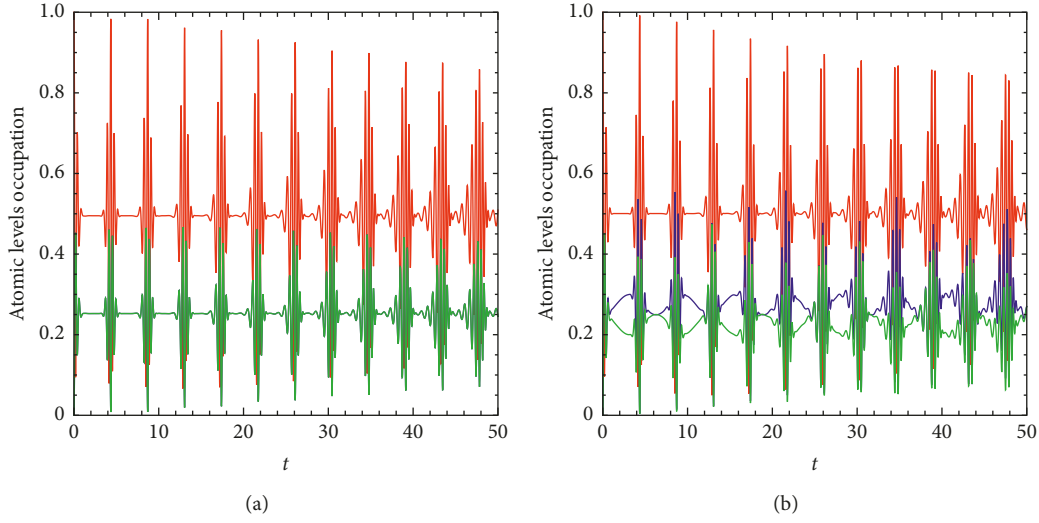


FIGURE 4: The evolution of the atomic levels occupation as a function of the scaled time t , with $\Delta_1 = 0.5, \Delta_2 = 0.5, \bar{\omega} = 0.5, q = 5, \xi = 10$. (a) $\tau = 0$, and (b) $\tau = 1$. $\rho_{11}(t)$ is represented by the red curve, $\rho_{22}(t)$ is represented by the blue curve, and $\rho_{33}(t)$ is represented by the green curve.

$$R_1(\hat{L}_y) = \frac{1}{2} (\wp_{11}(t) + \wp_{33}(t) + 2\text{Re}[\wp_{13}(t)]), \quad (47)$$

$$P_2(\hat{L}_y) = \frac{1}{4}\wp_{11}(t) + \frac{1}{2}\wp_{22}(t) + \frac{1}{4}\wp_{33}(t) + \frac{1}{\sqrt{2}}\text{Im}[\wp_{12}(t)] - \frac{1}{2}\text{Re}[\wp_{13}(t)] + \frac{1}{\sqrt{2}}\text{Im}[\wp_{23}(t)], \quad (48)$$

$$P_3(\hat{L}_y) = \frac{1}{4}\wp_{11}(t) + \frac{1}{2}\wp_{22}(t) - \frac{1}{\sqrt{2}}\text{Im}[\wp_{12}(t)] - \frac{1}{2}\text{Re}[\wp_{13}(t)] - \frac{1}{\sqrt{2}}\text{Im}[\wp_{23}(t)] + \frac{1}{4}\wp_{33}(t), \quad (49)$$

$$\begin{aligned} R_1(\hat{L}_z) &= \wp_{11}(t), \\ R_2(\hat{L}_z) &= \wp_{22}(t), \\ R_3(\hat{L}_z) &= \wp_{33}(t). \end{aligned} \quad (50)$$

Using the inequality (42), $H(\hat{L}_\beta)$ will satisfy the inequality.

$$H(\hat{L}_x) + H(\hat{L}_y) + H(\hat{L}_z) \geq 3 \ln 2. \quad (51)$$

If we put $\delta(\hat{L}_\beta) = \exp(H(\hat{L}_\beta))$, we obtain the following:

$$\delta H(\hat{L}_x) \delta H(\hat{L}_y) \delta H(\hat{L}_z) \geq 8. \quad (52)$$

The fluctuation in the components \hat{L}_β ($\beta = x$ or y) represents squeezing if $H(\hat{L}_\beta)$ satisfies the condition [25].

$$E(\hat{L}_\beta) = \left(\delta H(\hat{L}_\beta) - \frac{2\sqrt{2}}{\sqrt{|\delta H(\hat{L}_z)|}} \right) < 0, \quad \beta = x, y. \quad (53)$$

To study and analyze the periods of the entropy squeezing, the conditions mentioned above are used. When we exclude ECF and consider the resonance case, the squeezing intervals are achieved with respect to the first component x and never for the second component y . Moreover, the squeezing is found during the collapses regions and the beginning and end of revival regions. The absence of the ECF is because the functions $E(\hat{L}_x)$ and $E(\hat{L}_y)$ oscillate regularly, as shown in the Figure 5(a). When the nonresonance case is considered, the intervals of squeezing are reduced. The squeezing is generated in both x and y components alternately, as seen in Figure 5(b). The squeezing with respect to the y component disappears upon the insertion of the classical field. Squeezing improves the first component x significantly (see Figure 5(c)). Squeezing periods improved and became more pronounced with an increase in the influence of ECF, as observed in Figure 5(d).

5. Atomic Variables Squeezing

Now, we study the atomic variables squeezing. The uncertainty inequality for a three-level atom described by the angular momentum operators \hat{L}_x, \hat{L}_y , and \hat{L}_z is written as follows [31]:

$$\Delta \hat{L}_x \Delta \hat{L}_y \geq \frac{1}{2} |\langle \hat{L}_z \rangle|, \quad (54)$$

where \hat{L}_x, \hat{L}_y , and \hat{L}_z satisfy the commutation relation $[\hat{L}_x, \hat{L}_y] = i\hat{L}_z$.

The expectation values of \hat{L}_x, \hat{L}_y , and \hat{L}_z are given using the atomic reduced density matrix (40) in the following forms:

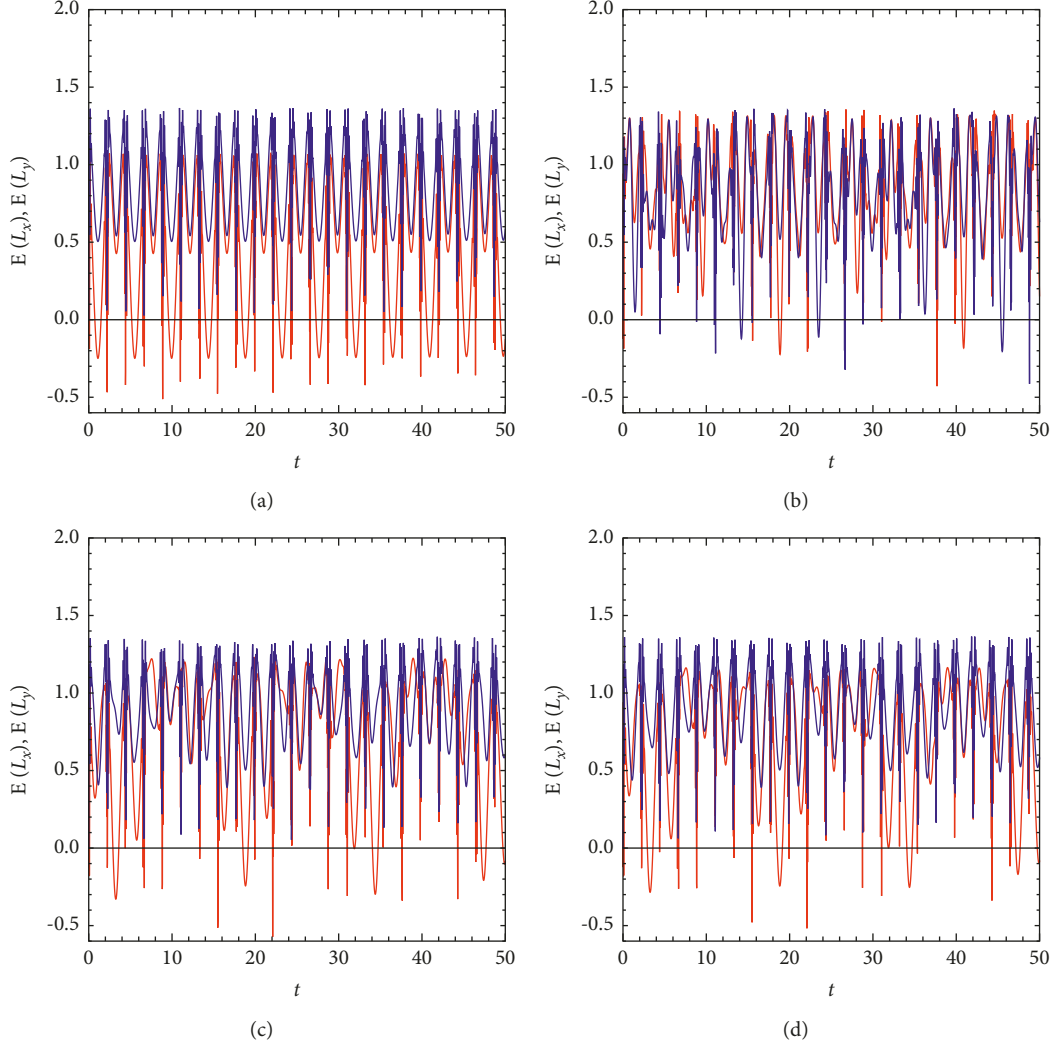


FIGURE 5: The components $E(\hat{L}_x)$ and $E(\hat{L}_y)$ as a function of the scaled time t , with $\omega = 1, q = 3, \xi = 16$. (a) $\Delta_1 = \Delta_2 = 0, \tau = 0$, (b) $\Delta_1 = 1, \Delta_2 = 2, \tau = 0$, (c) $\Delta_1 = 1, \Delta_2 = 2, \tau = 0.5$, (d) $\Delta_1 = 1, \Delta_2 = 2, \tau = 1$. The red curve represents $E(\hat{L}_x)$, and the blue curve represents $E(\hat{L}_y)$.

$$\langle \hat{L}_x \rangle = \frac{1}{\sqrt{2}} (\wp_{12}(t) + \wp_{21}(t) + \wp_{23}(t) + \wp_{32}(t)), \quad (55)$$

$$\langle \hat{L}_y \rangle = \frac{i}{\sqrt{2}} (-\wp_{12}(t) + \wp_{21}(t) - \wp_{23}(t) + \wp_{32}(t)), \quad (56)$$

$$\langle \hat{L}_z \rangle = \wp_{11}(t) - \wp_{33}(t). \quad (57)$$

The fluctuations in the component \hat{L}_β are squeezed if $\Delta\hat{L}_\beta$ satisfies the following condition:

$$V(\hat{L}_\beta) = \left(\Delta\hat{L}_\beta - \sqrt{\frac{\langle \hat{L}_z \rangle}{2}} \right) < 0, \quad \beta = x \text{ or } y, \quad (58)$$

where

$$\Delta\hat{L}_\beta = \sqrt{\langle \hat{L}_\beta^2 \rangle - \langle \hat{L}_\beta \rangle^2}. \quad (59)$$

with

$$\langle \hat{L}_x^2 \rangle = \frac{1}{2} [\wp_{11}(t) + \wp_{13}(t) + 2\wp_{22}(t) + \wp_{31}(t) + \wp_{33}(t)], \quad (60)$$

$$\langle \hat{L}_y^2 \rangle = \frac{1}{2} [\wp_{11}(t) - \wp_{13}(t) + 2\wp_{22}(t) - \wp_{31}(t) + \wp_{33}(t)], \quad (61)$$

$$\langle \hat{L}_z^2 \rangle = [\wp_{11}(t) + \wp_{33}(t)]. \quad (62)$$

This section is devoted to defining the atomic squeezing periods and comparing them with the entropy squeezing. In Figure 6(a), the ECF effect is neglected and the resonance case is considered. Squeezing is achieved by variable \hat{L}_x and not by \hat{L}_y . This result completely conforms with the entropy squeezing. Moreover, the squeezing occurs during the intervals of collapse. The intervals of squeezing decrease when the nonresonance case is inserted. It also shows a region of squeezing to the variable \hat{L}_y . However, considering the

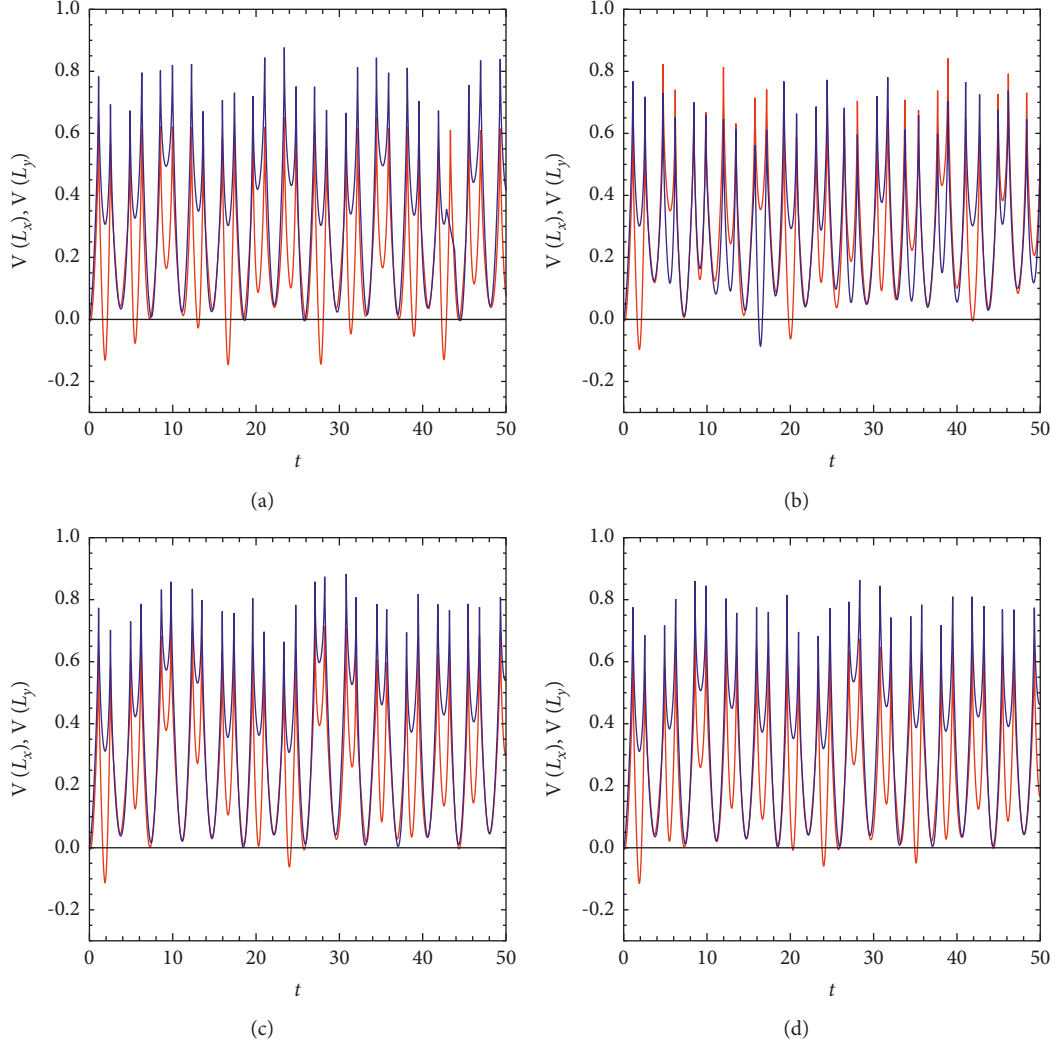


FIGURE 6: $V(\hat{L}_x)$ and $V(\hat{L}_y)$ as a function of the scaled time t . With $\omega = 0.3, q = 3, \xi = 0.5$. (a) $\Delta_1 = \Delta_2 = 0, \tau = 0$, (b) $\Delta_1 = 0.1, \Delta_2 = 0.2, \tau = 0$, (c) $\Delta_1 = 0.1, \Delta_2 = 0.2, \tau = 0.5$, (d) $\Delta_1 = 0.1, \Delta_2 = 0.2, \tau = 1$. $V(\hat{L}_x)$ is the red curve and $V(\hat{L}_y)$ is the blue curve.

nonresonance case leads to a reduction in the squeezing periods, as shown in Figure 6(b). The squeezing improves slightly for the variable \hat{L}_x after taking ECF into account. This improvement is more pronounced by increasing the influence of the ECF. Therefore, ECF plays an important role in the generating periods of squeezing (see Figures 6(c) and 6(d)).

6. Atomic Marginal Distribution

In this section, we study important nonclassical statistical properties, which is considered a hybrid between classical entropy and quantum mechanics. It is the atomic Wehrl density (AWD). It can be written as follows [32, 33]:

$$S_q(\theta, \phi, t) = -Q(\theta, \phi, t) \ln Q(\theta, \phi, t), \quad (63)$$

where $Q(\theta, \phi, t)$ is the atomic Q-function. For a three-level atom,

$$Q(\theta, \phi, t) = \frac{3}{4\pi} \langle \theta, \phi | \hat{\rho}_{\text{atom}}(t) | \theta, \phi \rangle, \quad (64)$$

where $|\theta, \phi\rangle$ is the atomic coherent state, which is written as follows:

$$\begin{aligned} |\theta, \phi\rangle = & \cos^2\left(\frac{\theta}{2}\right) |1\rangle + \sqrt{2} \cos\left(\frac{\theta}{2}\right) \sin\left(\frac{\theta}{2}\right) \exp(-i\phi) |2\rangle \\ & + \sin^2\left(\frac{\theta}{2}\right) \exp(-2i\phi) |3\rangle, \end{aligned} \quad (65)$$

where $0 \leq \theta \leq \pi$ and $0 \leq \phi \leq 2\pi$ indicate the atomic phase parameters. The marginal distribution of Q-function is given by integrating equation (64) over the variables θ .

The atomic marginal distribution $Q_\phi(t)$ is defined as follows:

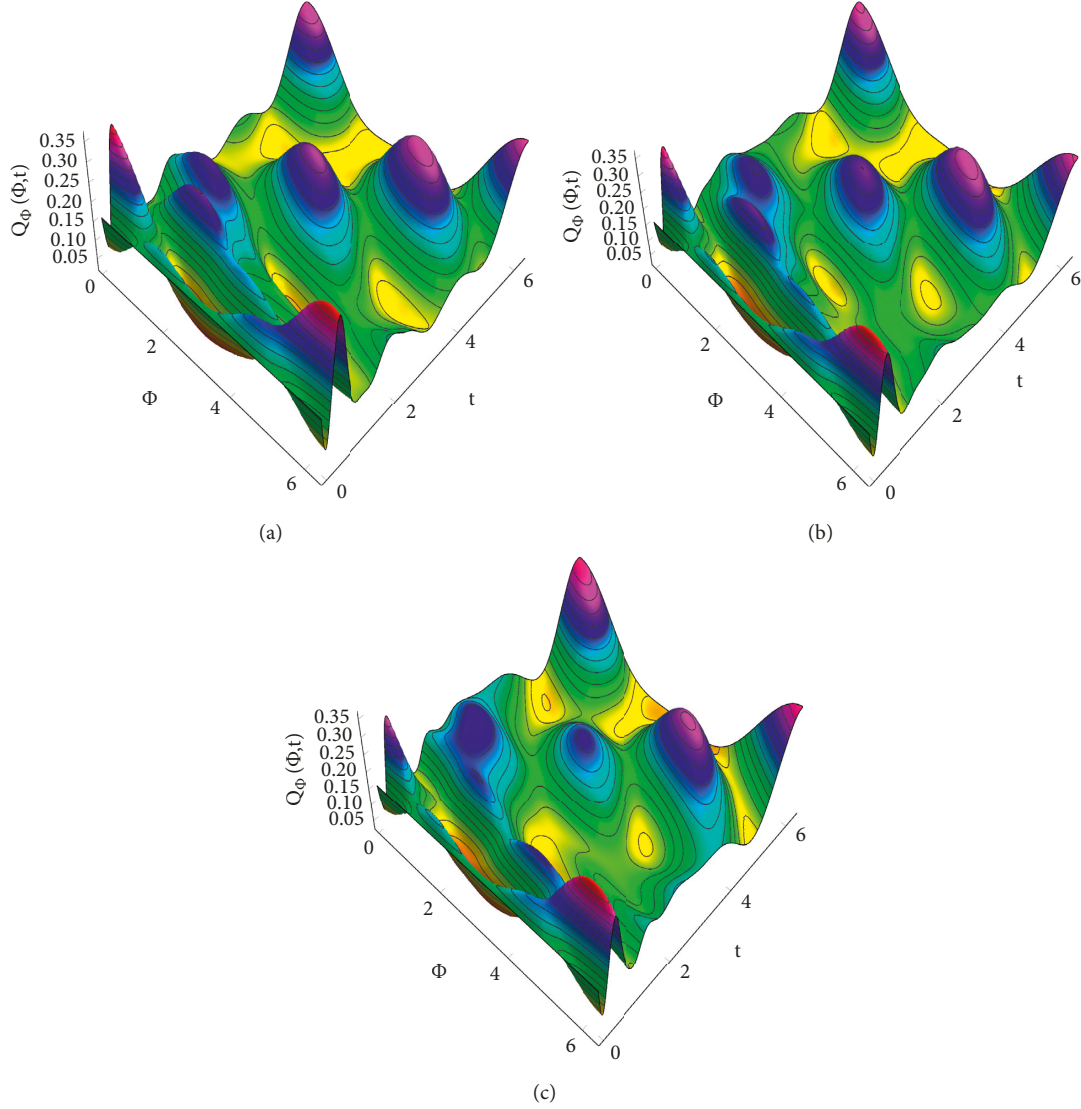


FIGURE 7: The marginal distribution $Q_\phi(t)$ as a function of the scaled time t with, $\omega = 0.2, q = 3, \xi = 16, \Delta_1 = 1, \Delta_2 = 2$, (a) $\tau = 0$, (b) $\tau = 0.5$, (c) $\tau = 1$.

$$\begin{aligned}
 Q_\phi(t) &= \int_0^\pi Q(\theta, \phi, t) \sin(\theta) d\theta \\
 &= \frac{1}{2\pi} (1 + \text{Re}[\wp_{13}(t) \exp(-2i\phi)]) \\
 &\quad + \frac{3}{8\sqrt{2}} \text{Re}[(\wp_{12}(t) + \wp_{23}(t)) \exp(-i\phi)].
 \end{aligned} \tag{66}$$

Using the aforementioned conditions in the atomic inversion, we neglect the effect of ECF. At the beginning of the interaction ($t = 0$), the marginal distribution $Q_\phi(t)$ begins with a peak that turns into a bottom by increasing the angle ϕ , followed by an improvement in the distribution until it reaches a peak at $\phi = 2\pi$. At $t = \pi$, the distribution begins with a bottom and then gradually improves until it reaches a peak at $\phi = \pi$, followed by a gradual decrease of the peak until it reaches the bottom at $\phi = 2\pi$. These phenomena are repeated every $t = 2\pi$ as shown in Figure 7(a). The

extreme values of the distribution function $Q_\phi(t)$ decrease after adding ECF $\tau = 0.5$. The effect of ECF is more obvious when taking $\tau = 1$, as shown in Figures. 7(b) and 7(c).

7. Conclusion

The influence of ECF is studied on a model describing the interaction of a three-level atom with a cavity filled with a two-mode field of an amplifier type. To obtain a solution to the Schrodinger equation, transformations between the atomic base are used. The effect of the classical field and detuning on atomic inversion, entropy squeezing, atomic variables squeezing, and the atomic marginal distribution are studied. The atom loses energy as a result of the detuning effect and is stationed in the ground states, whereas the atom stores energy as a result of the effect of the ECF on atomic inversion. The atom is in the excited state during most of the interaction period. The influence of ECF is more

pronounced when studying occupation for the second and third levels. The intervals of squeezing decrease when the nonresonance case is taken into account. The presence of ECF leads to improvement in the durations of squeezing in both entropy and variance squeezing. Therefore, ECF plays an important role in improving the energy storage of the atom. Squeezing periods improved and became more pronounced with an increase in the influence of ECF. The extreme values of the marginal distribution $Q_\phi(t)$ are reduced by the inclusion of ECF.

Data Availability

The data used in the study are generated from the measures in the article.

Conflicts of Interest

The authors declare that they have no conflicts of interest.

Acknowledgments

This research was supported by Taif University Researchers, Saudi Arabia Supporting Project Number: TURSP-2020/17, Taif University, Taif, Saudi Arabia.

References

- [1] E. T. Jaynes and F. W. Cummings, "Comparison of quantum and semi-classical radiation theories with application to the beam maser," *Proceedings of the IEEE*, vol. 51, no. 1, pp. 89–109, 1963.
- [2] A. Boca, R. Miller, K. M. Birnbaum, A. D. Boozer, J. Mckeever, and H. J. Kimble, "Observation of the vacuum rabi spectrum for one trapped atom," *Physical Review Letters*, vol. 93, no. 23, Article ID 233603, 2004.
- [3] A. M. Abdel-Hafez, A.-S. F. Obada, and M. M. A. Ahmad, "N-level atom and (N-1) modes: an exactly solvable model with detuning and multiphotons," *Journal of Physics A: Mathematical and General*, vol. 20, no. 6, pp. 359–L364, 1987.
- [4] N. H. Abdel-Wahab, "A three-level atom interacting with a single mode cavity field: different configurations," *Physica Scripta*, vol. 76, no. 3, pp. 244–248, 2007.
- [5] N. H. Abd El-Wahab, A. S. Abdel Rady, A.-N. A. Osman, and A. Salah, "A Study of three-level atom with one-mode cavity field in the presence of time-dependent coupling parameter and Kerr-like medium," *Middle-East Journal of Scientific Research*, vol. 23, p. 1532, 2015.
- [6] R. Daneshmand and M. K. Tavassoly, "The effects of damping on the approximate teleportation and nonclassical properties in the atom-field interaction," *The European Physical Journal D*, vol. 70, no. 5, p. 101, 2016.
- [7] L. Huai-xin and W. Xiao-qin, "Multiphoton Jaynes-Cummings model solved via supersymmetric unitary transformation," *Chinese Physics*, vol. 9, no. 8, pp. 568–571, 2000.
- [8] E. I. Aliskenderov, K. A. Rustamov, A. S. Shumovsky, and T. Quang, "On the Jaynes-Cummings model with multiphoton transitions in a cavity," *Journal of Physics A: Mathematical and General*, vol. 20, no. 18, pp. 6265–6270, 1987.
- [9] G. S. Agarwal, "Nonclassical statistics of fields in pair coherent states," *Journal of the Optical Society of America B*, vol. 5, p. 1940, 1988.
- [10] M. Abdel-Aty and A.-S. F. Obada, "Engineering entanglement of a general three-level system interacting with a correlated two-mode nonlinear coherent state," *The European Physical Journal D (EPJ D) - Atomic, Molecular and Optical Physics*, vol. 23, no. 1, pp. 155–165, 2003.
- [11] Z. Ke and F. Mao-fa, "Quantum entanglement in the system of two two-level atoms interacting with a single-mode vacuum field," *Chinese Physics*, vol. 14, pp. 2009–2013, 2005.
- [12] S. Abdel-Khalek, "Quantum Fisher information flow and entanglement in pair coherent states," *Optical and Quantum Electronics*, vol. 46, no. 8, pp. 1055–1064, 2014.
- [13] B. Mojaveri, A. Dehghani, M. A. Fasihi, and T. Mohammadpour, "Ground state and thermal entanglement between two two-level atoms interacting with a non-degenerate parametric amplifier: different sub-spaces," *International Journal of Modern Physics B*, vol. 33, no. 06, Article ID 1950035, 2019.
- [14] B. Mojaveri, A. Dehghani, M. A. Fasihi, and T. Mohammadpour, "Thermal entanglement between two two-level atoms in a two-photon Jaynes-Cummings model with an added Kerr medium," *International Journal of Theoretical Physics*, vol. 57, no. 11, pp. 3396–3409, 2018.
- [15] G. A. Abovyan and G. Y. Kryuchkyan, "Atomic deflection conditioned by entangled light waves," *Journal of Physics B: Atomic, Molecular and Optical Physics*, vol. 44, Article ID 045502, 2011.
- [16] R. Kumar, S. Sahoo, E. Joanni et al., "A review on synthesis of graphene, h-BN and MoS2 for energy storage applications: recent progress and perspectives," *Nano Research*, vol. 12, 2019.
- [17] K. Eckert, J. Mompart, R. Corbalán, M. Lewenstein, and G. Birkel, "Three level atom optics in dipole traps and waveguides," *Optics Communications*, vol. 264, no. 2, pp. 264–270, 2006.
- [18] J. Dalibard, F. Gerbier, G. Juzeliūnas, and P. Öhberg, "Colloquium: artificial gauge potentials for neutral atoms," *Reviews of Modern Physics*, vol. 83, no. 4, pp. 1523–1543, 2011.
- [19] T. M. El-Shahat, S. Abdel-Khalek, and A.-S. F. Obada, "Entropy squeezing of a driven two-level atom in a cavity with injected squeezed vacuum," *Chaos, Solitons & Fractals*, vol. 26, p. 1293, 2005.
- [20] M. S. Abdalla, E. M. Khalil, and A.-S. F. Obada, "Exact treatment of the Jaynes-Cummings model under the action of an external classical field," *Annals of Physics*, vol. 326, no. 9, pp. 2486–2498, 2011.
- [21] M. S. Abdalla, A.-S. F. Obada, E. M. Khalil, and S. I. Ali, "The influence of phase damping on a two-level atom in the presence of the classical laser field," *Laser Physics*, vol. 23, no. 11, Article ID 115201, 2013.
- [22] M. S. Abdalla, M. M. A. Ahmed, E. M. Khalil, and A.-S. F. Obada, "Entanglement between a single two-level atom and quantum systems of N-level atoms in the presence of an external classical field," *Journal of Russian Laser Research*, vol. 37, pp. 361–373, 2016.
- [23] M. Y. Abd-Rabbou, E. M. Khalil, M. M. A. Ahmed, and A.-S. F. Obada, "External classical field and damping effects on a moving two level atom in a cavity field interaction with Kerr-like medium," *International Journal of Theoretical Physics*, vol. 58, no. 12, pp. 4012–4024, 2019.
- [24] E. M. A. Hilal, S. Alkhateeb, S. Abdel-Khalek, E. M. Khalil, and A. A. Almowalled, "Quantum scheme for N-level atom interacting with a two two-level atom: atomic Fisher information and entropy squeezing," *Alexandria Engineering Journal*, vol. 59, no. 3, pp. 1259–1264, 2020.

- [25] A.-S. F. Obada, N. A. Alshehri, E. M. Khalil, S. Abdel-Khalek, and H. F. Habeba, "Entropy squeezing and atomic Wehrl density for the interaction between $SU(1, 1)$ Lie algebra and a three-level atom in presence of laser field," *Results in Physics*, vol. 30, 2021.
- [26] B. Mojaveri, A. Dehghani, Z. Ahmadi, and S. Amiri Faseghandis, "Interaction of a para-Bose state with two two-level atoms: control of dissipation by a local classical field," *The European Physical Journal Plus*, vol. 135, no. 2, p. 227, 2020.
- [27] A. Dehghani, B. Mojaveri, R. J. Bahrbeig, F. Nosrati, and R. L. Franco, "Entanglement transfer in a noisy cavity network with parity-deformed fields," *Journal of the Optical Society of America B*, vol. 36, no. 7, p. 1858, 2019.
- [28] J. Sánchez-Ruiz, "Improved bounds in the entropic uncertainty and certainty relations for complementary observables," *Physics Letters A*, vol. 201, no. 2-3, pp. 125–131, 1995.
- [29] J. Sánchez-Ruiz, "Asymptotic formula for the quantum entropy of position in energy eigenstates," *Physics Letters A*, vol. 226, no. 1-2, pp. 7–13, 1997.
- [30] C.-Y. Zhang and M.-F. Fang, "Entropy squeezing for a V -type three-level atom interacting with a single-mode field and passing through the amplitude damping channel with weak measurement," *Chinese Physics B*, vol. 30, Article ID 010303, 2021.
- [31] A.-S. F. Obada, M. M. A. Ahmed, M. Abu-Shady, E. M. Khalil, A.-B. A. Mohamed, and H. F. Habeba, "A nonlinear interaction between $SU(1, 1)$ quantum system and a three-level atom in different configurations with damping term," *Physica Scripta*, vol. 96, no. 4, Article ID 045105, 2021.
- [32] A. Wehrl, "On the relation between classical and quantum-mechanical entropy," *Reports on Mathematical Physics*, vol. 16, no. 3, pp. 353–358, 1979.
- [33] S. Abdel-Khalek and A.-S. F. Obada, "The atomic Wehrl entropy of a V -type three-level atom interaction with two-mode squeezed vacuum state," *Journal of Russian Laser Research*, vol. 30, 2009.